PREDICTION OF SOUND PRESSURE FIELDS BY PICARD-ITERATIVE BEM BASED ON HOLOGRAPHIC INTERFEROMETRY

H. Klingele and H. Steinbichler
Labor Dr. Steinbichler
Am Bauhof 4, D-83115 Neubeuern
Germany

ABSTRACT

Holographic interferometry offers amplitude data with a high spatial resolution which can be used as vibration boundary condition for calculating the corresponding sound pressure field. When investigating objects with arbitrary 3D-shape this requires contour measuring, performing holographic interferometry for three axes of freedom, combining contour and vibration data into a Boundary Element (BE) model, and then solving the discretized Helmholtz-Kirchhoff integral equation for the surface sound pressure. The latter is done by means of a newly developed Picard-iterative Boundary Element Method (PIBEM), which does not need matrix operations at all and such is capable of also treating large BE models arising from small bending wavelengths at high vibration frequencies. An experimental verification of this method by microphone measurements in an anechoic chamber is presented for a cylindrical example object.

1. HOLOGRAPHIC MEASUREMENT OF 3D-VIBRATION

In both pulse holography and electronic speckle pattern interferometry (ESPI) the measurement of the threedimensional vector of displacement $\vec{s}(x, y)$ is possible by introducing three directions $\vec{l}_i$ of illumination (see e.g. [1]). Fig. 1 shows the orientation of the corresponding sensitivity vectors $\vec{e}_i$. The apparent displacements measured by the interferograms i are the projections $\delta_i = \vec{e}_i\,\vec{s}$. Assembling the sensitivity matrix $\mathbf{E}$ from the $\vec{e}_i$ and solving for the actual displacement vector yields $\vec{s} = \mathbf{E}^{-1}\,\vec{\delta}$.

Here a 3D-ESPI system was used [2], since only stationary sinusoidal vibrations were considered for the following investigations of a test object. This object, a hollow metal tube with 200 mm diameter, 150 mm height, and 5 mm wall thickness was clamped to a thick steel plate at the bottom side. The vibration modes could be excited by a shaker attached inside the tube (Fig. 2).

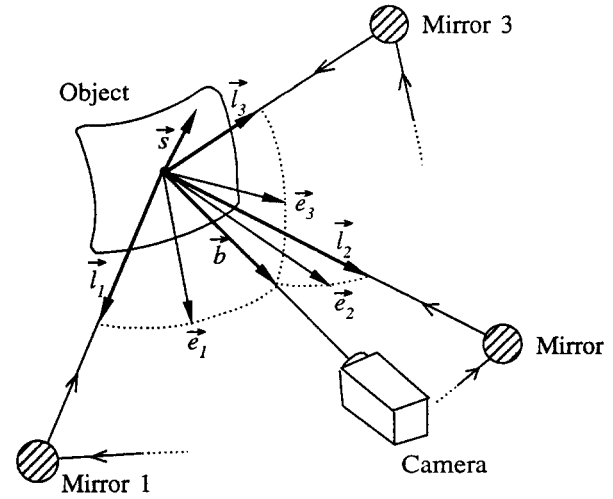

Figure 1: Setup for holographic measurement of 3D vibration.

Interferograms of the tube were taken directly with the CCD camera from four sides every 90^0, while the excitation force was fixed at the eigenfrequency $\nu = 2436$ Hz. For the quantitative evaluation of vibration amplitudes from the interferograms well-known methods like phase shifting and phase unwrapping were available by using the FRAMES image processing system [3].

2. CONTOUR MEASUREMENT AND MODELING

Advanced contour measurement setups based on projected fringes yield the absolute coordinates $z(x, y)$ of all object points appearing in the image by using triangulation methods. Here the TRICOLITE system [4]

0-7803-2431-5/95 $4.00

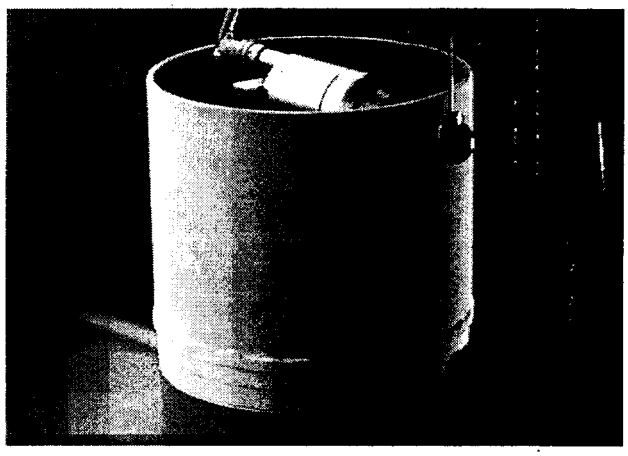

Figure 2: Metal tube with integrated shaker.

was applied, where the fringes are projected through a LCD mask.

To reduce the large amount of image data a surface mesh is generated on the contour images $z(x, y)$. It starts from a rectangular grid with a suitable maximum grid spacing and can be refined step-by-step dependent on surface curvature. The surface is then described by rectangles which are further split into flat triangle elements. Nodal points are defined by gridline crossings. To complete this Boundary Element description, the threedimensional displacement vectors from the evaluated interferogram images must be added to the surface mesh at the nodal points. This superposition of $z(x, y)$ and $\vec{s}(x, y)$ is straightforward if the same camera position is used for contour measurement and holography, which is possible when combining 3D-ESPI and TRICOLITE.

Contour and displacement may be measured and superimposed in the same way for some other camera positions in order to obtain a more complete BE description for the object under investigation. Tools were developed to concatenate two partial views of the surface, including the fitting of the surface parts, removal of overlapping elements, closing remaining gaps, and renumbering of nodal points and elements (Fig. 3). More than two partial views can be concatenated by repeated application of the two parts connection algorithm.

All the modeling actions described above were used to get a BE model for the tube under consideration from the four partial views of both contour and vibration. The result is displayed in a vector representation in Fig. 4.

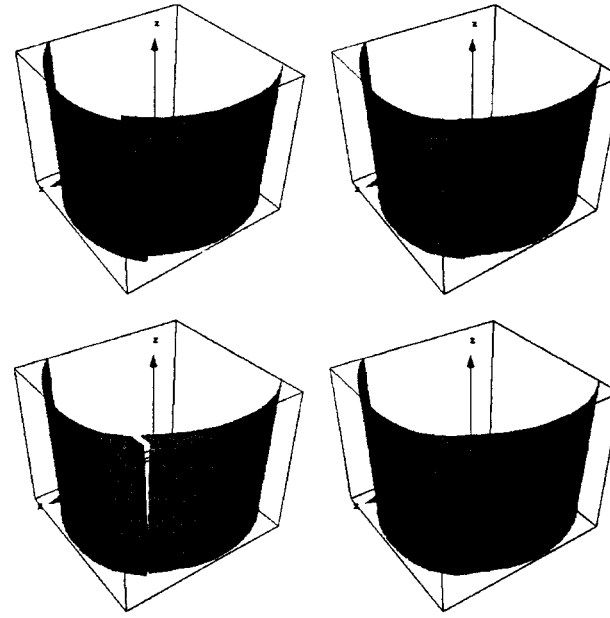

Figure 3: Connection of two BE models: initial state (upper left), surface fitting (upper right), removal of overlaps (lower left), closing remaining gap (lower right).

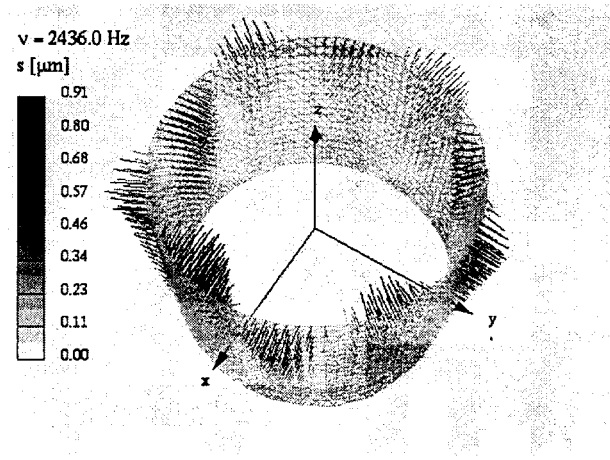

Figure 4: Vector representation of the vibration mode at $\nu = 2436$ Hz on the tube

3. SOUND CALCULATION

For the calculation of sound radiation from curved objects the Helmholtz-Kirchhoff integral formulation for the sound pressure $p(\vec{r})$ is usually applied [5]. Its general form for harmonic time dependence $e^{-i\omega t}$ is

$$\alpha\, p(\vec{r}) = \int_S p(\vec{r}_0)\frac{\partial G_k(\vec{r},\vec{r}_0)}{\partial n(\vec{r}_0)}\, dS(\vec{r}_0) - \int_S G_k(\vec{r},\vec{r}_0)\frac{\partial p(\vec{r}_0)}{\partial n(\vec{r}_0)}\, dS(\vec{r}_0) \qquad (1)$$

where the values $\alpha = 0, 1/2$, and 1 correspond to $\vec{r} \in V^-, S$, and V^+. The Greens function $G_k(\vec{r},\vec{r}_0)$ is given by

$$G_k(\vec{r},\vec{r}_0) = \frac{e^{ikR}}{4\pi R} \quad , \quad R = |\vec{r} - \vec{r}_0| \qquad (2)$$

with $k = \omega/c$. Fig. 5 depicts the geometry of the exterior acoustic radiation problem ($\alpha = 1$). The surface

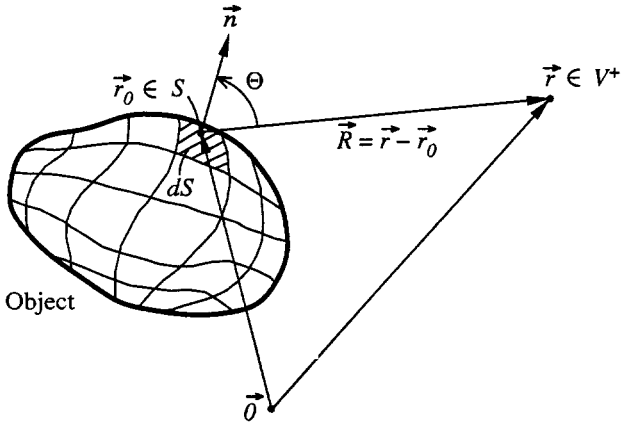

Figure 5: Geometry of the exterior acoustic radiation problem.

vibration measured by holography gives the Neumann boundary condition

$$\frac{\partial p(\vec{r}_0)}{\partial n(\vec{r}_0)} = \rho_0\, \omega^2 s_n(\vec{r}_0) \qquad (3)$$

where $s_n(\vec{r}_0)$ is the surface normal component of the displacement vector $\vec{s}(\vec{r}_0)$, and ρ_0 is the density of air. The unknown surface pressure $p(\vec{r}_0)$ is the second boundary condition appearing in the Helmholtz integral. It must be calculated by solving the integral equation for $p(\vec{r}_0)$ on the surface ($\alpha = 1/2$). The Helmholtz integral equation can now be rewritten in a discretized form by using collocation points i (being identical to the nodal points here) and introducing an integral operator $\mathbf{L}$ which performs the integrations over the surface pressure distribution

$$\frac{1}{2}\, p_i = \mathbf{L}\, p_i + f_i \qquad (4)$$

The f_i contain the direct integrations over the Neumann boundary condition (Eq. 3).

Contrary to the customary BEM solution procedure (setting up a linear system of equations from Eq. 4 and using Gaussian elimination, multigrid or conjugate gradient methods to solve it [6]) a Picard iterative algorithm (PIBEM) is proposed here. Starting from Eq. 4, the following general iteration formulation can be stated

$$p_i^{(n+1)} = a\,(\mathbf{L}\, p_i^{(n)} + f_i) + b\, p_i^{(n)} \qquad (5)$$

where $b = 1 - a/2$. Values of a in the range from about 0.1 to 1.0 yield convergent solutions (except for critical frequencies, see [6]). With the PIBEM method it is not necessary to set up and handle a matrix, because integrations are performed repeatedly in every iteration step. This allows to handle a large number of collocation points: a BE-model with about 14000 nodal points has already been solved.

As soon as the surface pressure has been calculated, the sound pressure in any point of the exterior region of the object (V^+) can be evaluated by means of the exterior Helmholtz integral ($\alpha = 1$). In Fig. 6 the result of the sound calculation is shown for the vibration mode on the tube already introduced in Fig. 4.

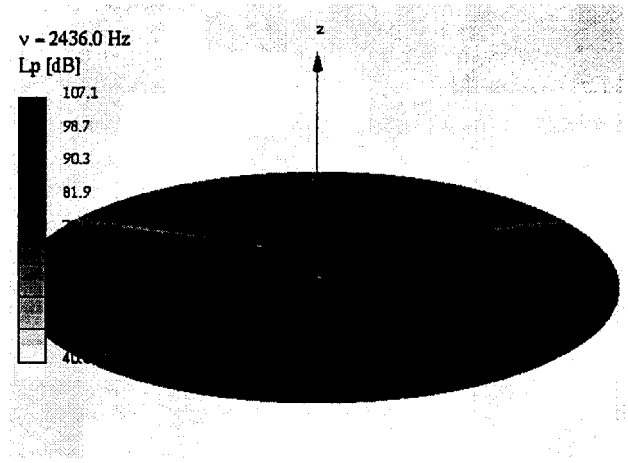

Figure 6: Sound pressure field around the tube.

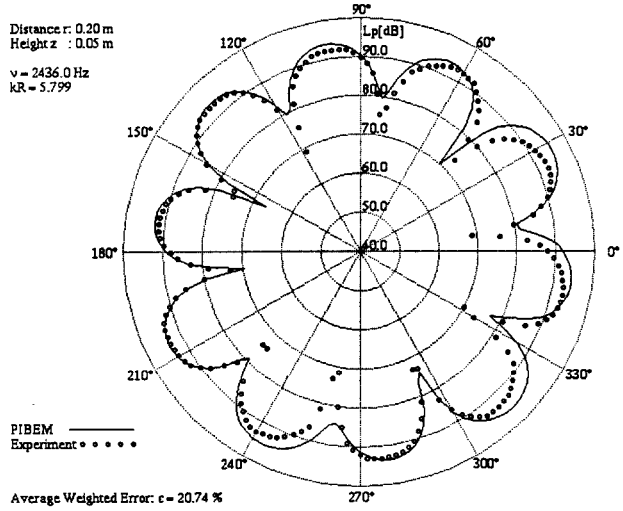

Figure 7: Comparison PIBEM vs. microphone measurement at $\nu = 2436$ Hz, $r = 0.2$ m, $z = 0.05$ m.

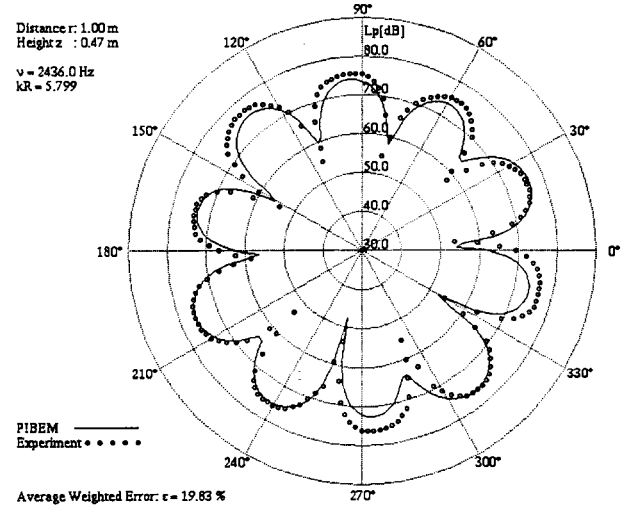

Figure 8: Comparison PIBEM vs. microphone measurement at $\nu = 2436$ Hz, $r = 1.0$ m, $z = 0.47$ m.

4. EXPERIMENTAL VERIFICATION

In order to verify the entire procedure of contour measurement, holography, BE-modeling and PIBEM calculation, the sound pressure field around the vibrating tube introduced in the previous sections was measured with a microphone in an anechoic chamber (University of Technology Munich, Prof. M. Lang). The shaker excitation was set to the same force and frequency as it was during taking the holographic interferograms. Fig. 7 shows the sound directivity plots resulting from measurement and calculation for the near field ($r = 0.2$ m, $z = 0.05$ m), Fig. 8 is the result along a more distant trace ($r = 1.0$ m, $z = 0.47$ m). Over large angular regions of the curves the aberration is of the order of 1 dB, which is on the other hand a useful accuracy for technical acoustics.

ACKNOWLEDGEMENTS

We wish to thank Prof. M. Lang for his technical and organizational support, H. Schmid for supervising the microphone measurements, and H. Zens for the evaluation of numerous holographic interferograms.

REFERENCES

[1] H. Marwitz (Ed.): *Praxis der Holographie*, expert-Verlag (1990).

[2] User manual for the 3D-ESPI System, Steinbichler Optotechnik GmbH (1994).

[3] User manual for FRAMES (Fringe Analysis and Measuring System), Steinbichler Optotechnik GmbH (1994).

[4] User manual for TRICOLITE (Triangulation with Coded Light), Steinbichler Optotechnik GmbH (1994).

[5] M. C. Junger, D. Feit: *Sound, Structures, and their Interaction*, MIT Press (1986).

[6] R. D. Ciskowski, C. A. Brebbia (Eds.): *Boundary Element Methods in Acoustics*, Computational Mechanics Publications (1991).